The Astrophysical Journal, 826:226 (10pp), 2016 August 1 doi:10.3847/0004-637X/826/2/226
© 2016. The American Astronomical Society. All rights reserved.

HOW SOFT GAMMA REPEATERS MIGHT MAKE FAST RADIO BURSTS

J. I. Katz
Department of Physics and McDonnell Center for the Space Sciences, Washington University, St. Louis, Mo. 63130, USA; katz@wuphys.wustl.edu
Received 2016 April 7; revised 2016 May 11; accepted 2016 May 24; published 2016 August 2

ABSTRACT

There are several phenomenological similarities between soft gamma repeaters (SGRs) and fast radio bursts (FRBs), including duty factors, timescales, and repetition. The sudden release of magnetic energy in a neutron star magnetosphere, as in popular models of SGRs, can meet the energy requirements of FRBs, but requires both the presence of magnetospheric plasma, in order for dissipation to occur in a transparent region, and a mechanism for releasing much of that energy quickly. FRB sources and SGRs are distinguished by long-lived (up to thousands of years) current-carrying coronal arches remaining from the formation of the young neutron star, and their decay ends the phase of SGR/AXP/FRB activity even though "magnetar" fields may persist. Runaway increases in resistance when the current density exceeds a threshold, releases magnetostatic energy in a sudden burst, and produces high brightness GHz emission of FRB by a coherent process. SGRs are produced when released energy thermalizes as an equlibrium pair plasma. The failures of some alternative FRB models and the non-detection of SGR 1806-20 at radio frequencies are discussed in the appendices.

Key words: plasmas – radiation mechanisms: non-thermal – radio continuum: general

1. INTRODUCTION

Fast radio bursts (FRBs) and soft gamma repeaters (SGRs) are rare and brief episodic events. Many authors (Popov & Postnov 2007, 2013; Kulkarni et al. 2014; Lyubarsky 2014; Kulkarni et al. 2015; Pen & Connor 2016; Katz 2016) have noted this similarity and have suggested that FRBs and SGRs may be associated. This paper considers the physical processes that may make FRBs from the sudden release of magnetic energy, which is believed to power SGRs. FRBs are, even at "cosmological" distances, $\sim 10^{-4}$ as powerful as the most powerful SGRs, so a process that makes FRBs from SGRs need not be efficient.

The recent discovery (Masui et al. 2015) of linear polarization and Faraday rotation in one FRB strengthens the case for cosmological distances. The measured rotation measure of FRB 110523 was $-186\ \mathrm{rad\ m^{-2}}$, implying the line-of-sight integral

$$\int n_e B_\parallel \, d\ell = 229\ \mathrm{pc}\ \mu\mathrm{G}\ \mathrm{cm}^{-3}. \quad (1)$$

Comparing to its dispersion measure of 623 pc cm^{-3} yields the electron density-averaged parallel field along the line of sight

$$\langle B_\parallel \rangle_{n_e} \equiv \frac{\int n_e B_\parallel \, d\ell}{\int n_e \, d\ell} = 0.37\ \mu\mathrm{G}. \quad (2)$$

This is more than an order of magnitude less than typical spiral galaxy fields $\sim 10\ \mu$G (Widrow 2002), and several orders of magnitude less than plausible fields in dense clouds or the immediate environments of stars. It indicates that the overwhelming majority of the dispersion occurs in the intergalactic medium, where nanogauss or weaker fields are expected and confirms the inference of "cosmological" distances. This implies that FRBs may have powers as great as $10^{43}\ \mathrm{erg\ s^{-1}}$ (Thornton et al. 2013), and requires correspondingly energetic sources. SGRs observed to have powers as high as $10^{47}\ \mathrm{erg\ s^{-1}}$ (Hurley et al. 2005) can satisfy this requirement.

It is generally accepted (Katz 1982, 1996; Thompson & Duncan 1992, 1995) that SGR outbursts result from the dissipation of magnetostatic energy in the magnetosphere of a highly magnetized neutron star (the "magnetar" model). Thompson & Duncan (1995) suggested that the rare giant flares of SGRs are produced by a rupture propagating across the entire solid crust, the general failure of a brittle object found in a model of brittle fracture (Katz 1986; Bak et al. 1987) now called "self organized criticality." Section 2 presents the phenomenological case for associating SGRs with FRBs. In Section 3, I apply the well-known theory of long-lived coronal currents in SGRs to FRBs. These currents are relics of neutron star formation, and their lifetimes are consistent with the inferred ages of SGRs and indicate that FRBs are similarly young. The presence of such magnetospheric currents distinguishes these magnetars from neutron stars in which currents are confined to the dense interior. Section 4 estimates the energy to which electrons are accelerated, which determines the decay time of the magnetospheric currents. Section 5 suggests a possible outburst mechanism and Section 6 considers curvature radiation as the emission mechanism of FRB, estimating the required charge clumping factor. Section 7 provides a brief summary and conclusion. Appendix A considers the hypothesis that Compton recoil of pair annihilation radiation may produce a plasma instability in the irradiated plasma, leading to large amplitude plasma waves that might produce high brightness GHz radiation; this hypothesis fails on energetic grounds. Appendix B considers some alternatives to the SGR hypothesis for FRBs at cosmological distances, specifically giant pulsar pulses and neutron star collapse and finds them wanting. Appendix C discusses the non-detection of an FRB in a radio observation (Tendulkar et al. 2016) fortuitously simultaneous with the giant outburst of SGR 1806-20 and suggests possible explanations.

2. THE CASE FOR ASSOCIATING SGRs AND FRBs

FRBs and SGRs have three distinct similarities that suggest an association.

1. Duty factor: their duty factors, defined as $D \equiv \langle F(t)\rangle^2/\langle F(t)^2\rangle$, where $F(t)$ is the flux, quantify the fraction of the time in which a source emits at close to its peak flux and are extremely low: $D \sim 10^{-10}$ for SGRs and $D < 10^{-8}$ for at least one FRB (Law et al. 2015).

2. Timescale: the intrinsic durations of FRBs have not been measured, but Thornton et al. (2013) found instrumentally limited upper bounds of about 1 ms for several FRBs. Some other FRBs have had widths of up to $\approx$10 ms that are attributed, because of their $\propto\nu^{-4}$ frequency dependence, to broadening by multipath propagation, and only upper bounds can be placed on the intrinsic pulse widths. This is consistent with the rise times of giant SGR outbursts. For instance, the rise time of the 1979 March 5 outburst of SGR 0525-66 was $<$200 μs (Cline 1980; Cline et al. 1980), Palmer et al. (2005) reported an exponential rise time of 300 μs for the giant 2004 December 27 outburst of SGR 1806-20, while their published data suggest a value of 200 μs, the giant 1998 August 27 flare of SGR 1900+14 had a rise time of $<$4 ms (Hurley et al. 1999), and earlier outbursts had rise times $\leqslant$8 ms (Mazets et al. 1979). These timescales are shorter than those of any other known astronomical event except gravitational wave emission by coalescing black holes and the pulses and subpulses of some pulsars; GRB durations and subpulse timescales are all $\gtrsim$30 ms (Fishman et al. 1994; Qin et al. 2013).

3. Repetition: SGRs repeat in complex irregular patterns, with periods of activity interspersed in longer periods of quiescence. The double pulse of FRB 121002, with subpulses separated by about 2 ms (Thornton 2013; Champion et al. 2015) may be considered a repetition, and multiple repetitions of FRB 121102 were recently discovered (Spitler et al. 2016) with irregular spacings reminiscent of the activity of SGR 1806-20 (Laros et al. 1987). FRBs are not catastrophic events that destroy their sources and resemble SGRs rather than GRBs.

3. THE MAGNETOSPHERE

It was realized soon after the discovery of the first SGR 0525–66 in 1979 that its combination of rapid rise ($<$200 μs) and energy release of 10^{44}–10^{45} erg (Cline 1980; Cline et al. 1980) required a source in a region of high-energy density. Magnetic reconnection (Priest & Forbes 2000) in the magnetosphere of a neutron star with (then) unprecedentedly strong magnetic fields was a natural model for the energy source (Katz 1982; Thompson & Duncan 1992, 1995).

In magnetic reconnection, magnetic energy is dissipated by resistive heating or particle acceleration in thin current sheets separating regions of differing, but comparatively homogeneous, magnetic fields. The current sheets may be modeled as resistors in series with an inductive energy store. If the electric field in the current sheets is large enough, counterstreaming electrons and ions (or positrons if they are present) make the plasma unstable to a variety of plasma waves. Correlated particles ("clumps") become effective scatterers, a condition described by an "anomalous" resistivity. This anomalous resistivity may be many orders of magnitude greater than the nominal resistivity resulting from interactions with uncorrelated particles.

The explosive growth of the resistivity ρ_e as a plasma instability exponentiates, while the current is held nearly constant by the circuit inductance, implies a proportionally explosive growth of the electric field $\boldsymbol{E} = \rho_e \boldsymbol{J}$ and of the dissipation rate $\boldsymbol{E}\cdot\boldsymbol{J} = \rho_e J^2$ (in large magnetic fields ρ_e, written here as a scalar, is a tensor, complicating the problem, but not changing the qualitative conclusion). The result can be rapid dissipation of large amounts of magnetostatic energy, depending on the evolution of ρ_e in space and time.

At energy fluxes $\gtrsim 10^{29}$ erg cm^{-2} s, such as those observed in giant SGR flares, the energy released thermalizes into an opaque equilibrium pair-blackbody photon gas, and a blackbody spectrum with a temperature of $\sim$20 keV is emitted (Katz 1996), roughly consistent with observed SGR spectra. Confinement of the charged particles by the magnetic field (Katz 1982; Thompson & Duncan 1995; Katz 1996) permits the radiated intensity to exceed the Eddington limit by large factors, as observed. Equilibration is expected during most of the $\sim$0.1 s duration of giant SGR flares. Their initial $<$1 ms rise times may correspond to the progress of a reconnection wave along a current sheet as plasma instability produces large amplitude charge clumps and increases resistivity by orders of magnitude.

Some positrons escape their source and annihilate in dense cooler matter such as the neutron star's surface, emitting characteristic annihilation radiation at energies of about 511 keV, as reported from SGR0525-66 (Cline 1980; Cline et al. 1980). It is natural to associate the $<$1 ms FRB with the $<$1 ms rise time of giant SGR flares, before the electron–positron pairs have had time to equilibrate as a lower temperature plasma, converting most of their rest mass energy into blackbody photons.

Idealized neutron stars have sharply defined radii, with thermal scale heights $\lesssim$1 cm after rapid early cooling. Above this scale height (unless they are accreting), the surrounding space is nearly a vacuum, filled only with a non-neutral plasma with the Goldreich–Julian density (Davis 1947; Hones & Bergeson 1965; Goldreich & Julian 1969)

$$n_{\rm GJ} = -\frac{\boldsymbol{\omega}_{\rm rot}\cdot\boldsymbol{B}}{2\pi ce} \tag{3}$$

for an aligned magnetic dipole field and rotation rate $\omega_{\rm rot}$. The defining characteristic of "magnetar" models is the assumption that rotation is unimportant: their radiation is derived from their magnetostatic energy, $n_{\rm GJ}$ is insignificant and (except for rotational modulation of the observed radiation) the star may be considered non-rotating.

This leads to questions regarding magnetar models of FRBs: magnetic reconnection is implausible in the neutron star interior for which high density implies high conductivity and low electron-ion drift velocity. This precludes plasma instability and the development of anomalous (turbulent) resistivity, the generally accepted mechanism of magnetic reconnection (Priest & Forbes 2000) in low density plasma. If reconnection were somehow to occur in the neutron star interior, it would only warm the dense matter there, with the released energy slowly diffusing to the surface to be radiated as thermal X-rays.

The electron-ion drift speed

$$v_{\rm drift} = \frac{J}{n_e e} \sim \frac{Bc}{4\pi r n_e e} \sim 10^4 \frac{B_{15}}{\rho_m}\ {\rm cm\ s^{-1}}, \tag{4}$$

where ρ_m is the mass density and $B_{15} \equiv B/(10^{15}\ {\rm G})$. Anomalous resistivity can only occur where $\rho_m \ll 1\ {\rm g\ cm^{-3}}$ in an optically thin atmosphere (which may not exist if magnetic

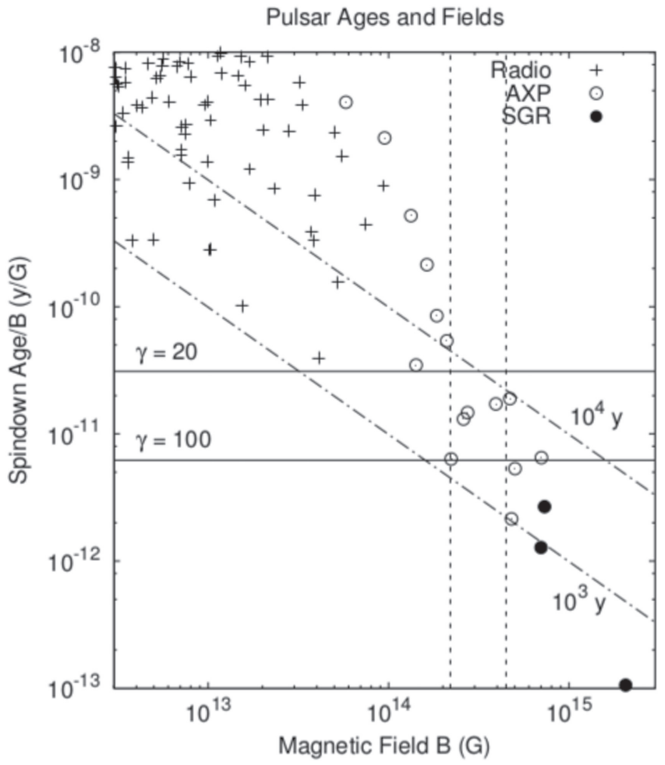

Figure 1. Spindown ages and magnetic fields of all objects in the ATNF Pulsar Catalog (Manchester et al. 2005) with parameters in the displayed range that are categorized as "radio but not AXPs" or "AXP." Of the "AXPs," only four (all with $2 \times 10^{14} < B < 3 \times 10^{14}$) have reported radio emission. The SGRs that have shown giant flares (SGR 0526-66, SGR 1806-20, and SGR 1900 +14) are categorized as "AXPs," but here are shown with a distinctive symbol. Diagonal dotted–dashed lines indicate spindown ages. Horizontal lines indicate the ratio of lifetime to B (plotted on the "Spindown Age/B" axis) corresponding to their value of γ. All "AXPs" lying below the $\gamma = 20$ line have $B > 2.2 \times 10^{14}$ G and all below the $\gamma = 100$ line have $B > 4.5 \times 10^{14}$ G; these fields are indicated by vertical dashed lines.

quantization of electron states gives neutron stars abrupt surfaces).

Rapidly rising SGR outbursts and FRBs must occur in nearly transparent regions (optical depth $\lesssim 1$) in order for their radiation to escape in their observed sub-millisecond rise times. However, reconnection cannot occur in a vacuum magnetosphere, despite its high magnetostatic energy density, because no currents flow in a vacuum. Here the theory (Thompson & Duncan 1992, 1995; Thompson et al. 2002; Beloborodov & Thompson 2007) of the magnetar origin of SGRs is applied to SGR models of FRBs.

These problems may be resolved if substantial portions of the neutron star's magnetic moment are produced by current loops flowing through long-lived quasi-neutral coronal arches above the high density neutron star surface. Actual force-free configurations (in magnetar fields, the cross-field conductivity is very small, electrons are in their quantized ground states, and any cross-field currents would imply enormous Lorentz forces, so that $\boldsymbol{J} \| \boldsymbol{B}$) are complex (Parker 1979; Akgün et al. 2016).

As a neutron star forms from the collapse of a stellar core, frozen-in magnetic fields are amplified by compression and possibly by turbulence. In the earlier stages of contraction, the matter pressure far exceeds the magnetic stress. Currents flow along the field lines, along which the conductivity is always higher than perpendicular to them (although at high densities there may also be cross-field currents). As the matter (radiating neutrinos) gradually settles into its final configuration, the magnetic stress becomes dominant in the low density regions above the developing neutron star surface, and the matter there is constrained to flow along the field lines. Magnetic field lines still penetrate that surface (if they did not, all multipole moments would be zero). The magnetosphere must be force-free, with $\boldsymbol{J} \| \boldsymbol{B}$, because pressure gradients are insufficient to oppose any Lorentz force and because the cross-field conductivity is low at low matter density. However, there is no reason to expect the parallel component of $\boldsymbol{J}$ to disappear during collapse.

The resulting picture is one of a magnetosphere in which, near the stellar surface

$$J \sim \frac{cB}{4\pi r} \sim 2 \times 10^{18} B_{15} \frac{\mathrm{esu}}{\mathrm{cm}^2\ \mathrm{s}}, \quad (5)$$

where B_{15} refers only to that portion of the field generated by magnetospheric currents.

Current flows on loops and produces a magnetic flux through a representative loop

$$\Phi \sim Br^2 \sim 10^{27} B_{15}\ \mathrm{G\ cm}^2. \quad (6)$$

Magnetospheric current loops of this sort have been considered by Thompson et al. (2002), Beloborodov & Thompson (2007), and Beloborodov (2009) as the origin of magnetar coronæ and by Lyutikov (2006, 2013) to explain SGR flares and magnetar "anti-glitches" if they open to infinity during flares, in analogy to solar coronal mass ejections.

The electromotive force (EMF) induced by the changing flux through the loop drives the current flow along the magnetic field lines. At one foot (B) of the arch, electrons are pulled out of the surface plasma and accelerated toward the other foot (A); positive ions (and possibly positrons) are pulled from the surface (A) and accelerated in the opposite direction. Both signs of charge carriers contribute to the current. Beloborodov & Thompson (2007) assumed only one positive charge carrier (or positive charge carriers all with the same charge to mass ratio) and found that no steady solution is possible and that pairs must be produced, but multiple positive ion species and ionization states are likely to be present. Our estimates average over any rapid variability for which the timescale is $\sim r/c \sim 30\ \mu$s, shorter even than SGR rise times and the upper bounds on FRB duration.

The current is mostly carried by relativistic electrons with density

$$n_e \sim \frac{J}{(1 + J_+/J_-)ce} \sim \frac{B}{4\pi re} \sim 2 \times 10^{17} B_{15}\ \mathrm{cm}^{-3}, \quad (7)$$

where J_+ and J_- are the current densities of positive and electron charge carriers, respectively; $J_+/J_- \leqslant 1$ because ions move more slowly than electrons. The electrons in the current loop must be quasi-neutralized by ions or positrons because, otherwise, their electrostatic field $E \sim n_e e r^3/r^2 \sim B/4\pi$ would be impossibly large.

This electron density may be compared to the co-rotation density (Equation (3)): $n_{\mathrm{GJ}}/n_e < 2\omega_{\mathrm{rot}} r/c$. The co-rotating charge density is insignificant except near the co-rotation radius, where the magnetic energy density and available power are very small.

The quasi-neutral low density current-carrying plasma is gravitationally attracted to the star and would slide down the magnetic field lines to the surface. However, n_e cannot fall below the value given by Equation (7) because that would interrupt the flow of the current, changing the flux through the loop and inducing an EMF sufficient to maintain the current.

The current-carrying electrons strike the star with a Lorentz factor γ, acquired in their descent from C to A by the electric field that lifts positive ions to maintain quasi-neutrality. The implied EMF is $\approx\gamma m_e c^2/e$ because contributions from the electric field on the arch between B and C and inside the star are small (electrons require little energy to lift from B to C and the stellar interior is an Ohmic conductor of high conductivity). Equating this EMF to $\partial\Phi/\partial(ct) \sim \Phi/c\tau \sim Br^2/c\tau$ yields the magnetic decay time τ:

$$\tau \sim \frac{r^2 eB}{\gamma m_e c^3} \sim 6 \times 10^5 \frac{B_{15}}{\gamma} \text{ year}. \quad (8)$$

Of course, only the component of field attributable to magnetospheric current decays on this timescale.

The ratio Age$/B$, where Age is the spin-down age, is plotted in Figure 1 for pulsars from the ATNF Pulsar Catalog (Manchester et al. 2005). This provides an estimate of γ for SGRs/AXPs for which the magnetospheric current contributes a substantial fraction of the slowing-down torque, but it has no such significance for ordinary radio pulsars whose magnetospheric currents have decayed. Pulsars categorized in the catalog as "radio but not AXP" are indicated as "Radio" while those categorized as "AXP" are indicated as "AXP" or (the three with observed giant flares) "SGR." Pulsars with smaller estimated fields (including most ordinary pulsars as well as millisecond pulsars) are not shown. It is likely that each category contains some incorrectly classified objects (e.g., accreting neutron stars or other X-ray pulsars misclassified as AXPs in the catalog).

The horizontal lines are upper bounds on the actual ages corresponding to the indicated values of γ. If the actual ages are close to the spindown ages, as is the case for pulsars that have spun down from much faster rotation at birth, then SGRs/FRBs will lie on or below the lines corresponding to their values of γ. They will be below these horizontal lines if their magnetospheric currents have decayed very little, possibly suggesting that the neutron star is in the early stages of its active life as an SGR/FRB. If its spindown age is greater than its actual age, a neutron star may lie above the horizontal line; however, the absence of points in the upper right part of the figure suggests that this is not common.

All radio pulsars lie above the $\gamma = 20$ line, suggesting that when SGRs reach the age τ they turn into radio pulsars even if their fields remain in the "magnetar" range. This is consistent with the hypothesis that SGRs must be younger than τ, and that any older object can only be a radio pulsar, however large its magnetic field. Every "AXP" in the Catalog above the $\gamma = 20$ line has $B \leqslant 2.2 \times 10^{14}$ G (indicated by a dashed line), and every "AXP" with $B \leqslant 2.2 \times 10^{14}$ is above the $\gamma = 20$ line. This 1:1 correspondence suggests that these objects form a population distinct from those of the higher-B, younger-aged "AXP," and may not be SGRs/AXPs at all.

The concentration of the SGRs with giant flares to the lower right corner of Figure 1 appears to be statistically significant. Of the five "AXPs" below the $\gamma = 100$ line, three are the SGRs with giant flares ($P = 0.024$) and these three are among the four "AXPs" with the highest Age$/B$ ($P = 0.011$). Although these statistics are a posteriori, they suggest that as SGRs age past τ they may remain AXPs as a result of magnetic dissipation within their interiors, but that their SGR activity decays along with their magnetospheric currents. Only a fraction of AXPs are SGRs, and the absence of SGR activity in most AXPs (those with greater ratios of age to field) is not an artefact of limited observations but an intrinsic property.

4. ELECTRON ENERGY

For a magnetic arch with a gravitational potential difference Ω between its top and the neutron star surface,

$$\int_A^C \boldsymbol{E} \cdot \boldsymbol{d\ell}_{\rm arch} = \Omega \frac{Am_p}{Ze} \sim \frac{GMm_p \delta r}{r^2 e} \frac{A}{Z} \quad (9)$$

is required to raise the neutralizing ions from A to the top of the arch (C) a height δr above the neutron star's surface, where the atomic number A, proton mass m_p, and ionization state Z describe the neutralizing ions. The electrons, closing their path to the stellar surface, acquire a kinetic energy $-e\int_C^A \boldsymbol{E} \cdot \boldsymbol{d\ell}_{\rm arch}$ that they dissipate in collisions in the star at A.

Above the surface of a cooling neutron star with a nominal surface blackbody temperature of ~0.1–1 keV iron may be ~20–24 times ionized, although less in strong magnetic fields that increase the ionization potentials. The plausible range of A/Z is from 1 (accreted hydrogen) to ~2–5 for strongly magnetized iron.

The magnetostatic energy available (in a dipole field) is $B^2R^3/6$ (Katz 1982) and the dissipated power is $B^2R^3/(6\tau) \sim 10^{34} B_{15} \gamma$ erg s^{-1} if the neutron star is young enough that much of its magnetic moment is produced by currents in loops that extend through the surface into the magnetosphere. After those loops decay, the stars will retain the magnetic moments produced by their internal currents. The same result is obtained, to order of magnitude, from Equation (5) if J is assumed to extend over the entire surface:

$$P \sim 4\pi r^2 n_e \gamma m_e c^3 \sim \frac{Br\gamma m_e c^3}{e} \sim 6 \times 10^{34} \gamma B_{15} \text{ erg s}^{-1}, \quad (10)$$

consistent with the steady (except for rotational modulation) X-ray emission from the heated surface. This power is in addition to that generated by magnetic dissipation in the stellar interior.

Equating the EMF (Equation (9)) to $\gamma m_e c^2/e$ and taking $\delta r = 3$ km,

$$\gamma \approx \frac{\Omega}{c^2} \frac{m_p}{m_e} \frac{A}{Z} \approx 40 \frac{A}{Z}, \quad (11)$$

with γ plausibly in the range 40–400. Substituting this into Equation (8) yields

$$\tau \sim \frac{r^2 eB}{m_p c \Omega} \frac{Z}{A} \sim 5000\ B_{15} \left(\frac{\delta r}{3 \text{ km}}\right)^{-1} \frac{Z}{A} \text{ year}. \quad (12)$$

5. OUTBURST MECHANISM

5.1. Plasma Instability?

The counterstreaming electron and ion currents would seem to invite the two-stream plasma instability (Chen 1974). This is unlikely to explain the outbursts.

1. The plasma frequency corresponding to the electron density of Equation (7) exceeds observed FRB frequencies by orders of magnitude, even allowing for the relativistic increase of mass with the Lorentz factor (11), so that oscillations of this plasma cannot emit the observed radiation.
2. The counter streaming currents are present at all times. An instability might produce steady emission, but there is no evident mechanism for it to make rare, low duty factor, giant outbursts.
3. The electrons are highly relativistic, moving with Lorentz factors $\gamma \gg 1$ exactly parallel to $\boldsymbol{B}$ because their transverse motion decays immediately in a quantizing magnetic field. Their response to the electric field of a longitudinal plasma wave with $\boldsymbol{E}\|\boldsymbol{B}$ is reduced by a factor γ^{-3} compared to that of non-relativistic electrons (their response to any transverse component of $\boldsymbol{E}$ is zero because the magnetic field is quantizing). This suppresses the growth of the two-stream instability (Melrose & Yuen 2016).

5.2. Coulomb Scattering

The scattering cross-section of the neutralizing ions for the current-carrying electrons may be estimated, though a quantitative calculation would require use of their wave-functions in the quantizing magnetic field. We assume that the electron motion is only parallel to the field and that the backscattering cross-section is the integral of the Mott cross-section in the relativistic limit, ignoring ionic recoil (ionic transverse motion is less strongly quantized even in "magnetar" fields), over the backward hemisphere:

$$\sigma = 2\pi \int_{-1}^{0} \frac{Z^2 e^4}{4\gamma^2 m_e^2 c^4} \csc^4(\theta/2) \cos^2(\theta/2)\, d\cos\theta = \pi(1 - \ln 2)\frac{Z^2 e^4}{\gamma^2 m_e^2 c^4} = 7.6 \times 10^{-26} \frac{Z^2}{\gamma^2}\ \mathrm{cm}^2. \quad (13)$$

Using the estimate (11) for γ

$$\sigma \sim 5 \times 10^{-29} \frac{Z^4}{A^2}\ \mathrm{cm}^2 \lesssim 7 \times 10^{-27}\ \mathrm{cm}^2, \quad (14)$$

where the upper bound is taken for completely ionized Fe ions.

The integrated column density of electrons along a coronal arch of length r is

$$n_e r \sim \frac{B}{4\pi e} \sim 2 \times 10^{23} B_{15}\ \mathrm{cm}^{-2}. \quad (15)$$

Assuming the current-carrying electrons are quasi-neutralized by ions (see below), the corresponding column density of ions is

$$n_i r = \frac{n_e r}{Z} \sim \frac{B}{4\pi e Z} \sim 2 \times 10^{23} \frac{B_{15}}{Z}\ \mathrm{cm}^{-2}. \quad (16)$$

Comparing to the cross-section, Equation (16) shows that the ionic Coulomb scattering probability P_{scatt} of the current-carrying electrons in the magnetospheric arch is negligible:

$$P_{\mathrm{scatt}} = n_i r \sigma \sim \frac{Z^2 e^4}{\gamma^2 m_e^2 c^4} \frac{B}{4\pi e Z} \sim \frac{1 - \ln 2}{4} B \frac{Z^3 e^3}{\Omega^2 m_p^2 A^2} \sim \frac{1 - \ln 2}{4} \frac{m_e^2 c^4}{\Omega^2 m_p^2} \alpha \frac{B}{B_c} \frac{Z^3}{A^2} \sim 3 \times 10^{-7} \frac{Z^3}{A^2} \frac{B_{15}}{\Omega_{20}^2} \ll 1, \quad (17)$$

where $B_c \equiv m_e^2 c^3/e\hbar = 4.413 \times 10^{13}\,\mathrm{G}$ is the quantum critical field, α is the fine-structure constant and $\Omega_{20} \equiv \Omega/(10^{20}\,\mathrm{erg\ g^{-1}})$. The electrons are ballistically accelerated by the electrostatic field that supports the neutralizing ions, and Ohmic resistivity is inapplicable.

5.3. A Possible Mechanism

Crustal and interior motions in the neutron star rearrange its surface magnetic field and the structure of its magnetosphere (Thompson & Duncan 1992, 1995). As a result, the current may, locally or globally, concentrate on sheets of thickness $h \ll r$. Concentration of currents on thin sheets occurs during magnetic reconnection (Priest & Forbes 2000). When contacting plates of highly conductive neutron star crust, with frozen-in fields, are displaced with respect to one another, volumes of magnetosphere with different fields may be brought into contact with the tangential magnetic discontinuity accommodated by a thin current sheet. In Equations (5) and (7), r is replaced by h, which may be very small, at least near the crustal plates. Equation (17) becomes

$$P_{\mathrm{scatt}} \sim \frac{1 - \ln 2}{4} \frac{m_e^2 c^4}{\Omega^2 m_p^2} \alpha \frac{Z^3}{A^2} \frac{B}{B_c} \frac{r}{h} \sim 3 \times 10^{-7} \frac{Z^3}{A^2} \frac{B_{15}}{\Omega_{20}^2} \frac{r}{h}. \quad (18)$$

When $P_{\mathrm{scatt}} \ll 1$, the resistivity is not Ohmic; most electron motion is ballistic. However, when $P_{\mathrm{scatt}} \gg 1$, the "scattering optical depth" of the coronal arch to the electrons is P_{scatt} and the electrons undergo a one-dimensional random walk (the only scattering possible is in the backward direction), reducing their mean speed to c/P_{scatt}. This increases the charge density required to carry the current density by the same factor of P_{scatt}, and quasi-neutrality multiplies the density of scatterers by that factor again. The result is a limiting current density set by the condition $P_{\mathrm{scatt}} \approx 1$:

$$J_{\max} \sim \frac{\Omega^2 m_p^2 c}{\pi(1 - \ln 2) e^3 r} \frac{A^2}{Z^3} \sim 8 \times 10^{24}\ \Omega_{20}^2 \frac{A^2}{Z^3}\ \frac{\mathrm{esu}}{\mathrm{cm^2\ s}} \sim 3 \times 10^{15}\ \Omega_{20}^2 \frac{A^2}{Z^3}\ \frac{\mathrm{A}}{\mathrm{cm^2\ s}}. \quad (19)$$

When the current density required by the magnetic field exceeds $J_{\max}$

$$\frac{c}{4\pi} \frac{B}{h} > J_{\max} \quad (20)$$

a condition found if

$$\frac{h}{r} < \frac{1-\ln 2}{4}\frac{Be^3}{\Omega^2 m_p^2}\frac{Z^3}{A^2} \sim 3\times 10^{-7}\frac{B_{15}}{\Omega_{20}^2}\frac{Z^3}{A^2}. \quad (21)$$

it becomes impossible for the current sheet to carry the current implied by the assumed magnetic configuration. It is difficult to be sure what the consequences will be, but it is plausible that the result will be a runaway increase in plasma density on the current sheet as the scattering and resistance increase and the rapid deposition of enough magnetic energy and the field configuration relaxes to one consistent with $J < J_{\max}$.

6. THE CLUMPING FACTOR

The extraordinary brightness of FRBs requires coherent emission. Katz (2014) estimated the degree of clumping for emission by relativistically expanding plasma, but in the present model the source is trapped in a neutron star magnetosphere, with zero bulk velocity. The angle-integrated spectral density emitted by a charge $N_e e$ moving with Lorentz factor $\gamma \gg 1$, integrated over the passage of its radiation pattern, is (Jackson 1962)

$$\frac{dI}{d\omega} \sim \frac{(N_e e)^2\gamma}{c}. \quad (22)$$

Adopting $\gamma = 100$, distributing the observed $\sim 10^{40}$ erg of the brightest FRBs (Thornton et al. 2013) over a spectral bandwidth $\sim 10^{10}$ s^{-1} and $\sim 10^{10}$ radiating "bunches" (coherent emission is only possible for sources whose dimensions are $< \lambda/2 \approx 10$ cm) and allowing for ~ 1 ms$/(r/c) \sim 30$ passages through a current sheet of dimension $\sim r$ yields $N_e \sim 6\times 10^{22}$.

This would imply a potential $V \sim N_e e/(\lambda/2) \sim 3 \times 10^{12}$ esu, or an electrostatic energy of 1.5×10^3 erg (10^6 GeV) per electron ($\gamma \sim 10^9$) and an electric field of 3×10^{11} cgs or 10^{14} V cm^{-1}. Such an electric field would be about 1% of the characteristic quantum field $E_c \equiv m_e^2 c^3/e\hbar$ (Heisenberg & Euler 1936; Schwinger 1951), approaching the threshold of "Schwinger sparks" at 5% of the characteristic field (Stebbins & Yoo 2015). However, these fields are inconsistent with the assumed $\gamma \sim 100$.

A self-consistent solution of Equation (22) and $\gamma m_e c^2 = N_e e^2/(\lambda/2)$ is

$$N_e = \left(\frac{dI}{d\omega}\frac{(\lambda/2)m_e c^3}{e^4}\right)^{1/3} \sim 2\times 10^{20}$$
$$\gamma \sim 10^7. \quad (23)$$

The electron energy $eV \sim 10^4$ GeV, about 100 times less than in the preceding paragraph.

These extraordinary numbers follow from the inferred brightness temperatures (and cosmological distances) of FRBs and are not specific to the model (Katz 2014); qualitatively similar inferences follow from the observation of nanosecond "nanoshots" of Galactic pulsars (Soglasnov et al. 2004; Hankins & Eilek 2007) whose sources must be as small as a few meters. Such electrostatic potentials imply much larger $\gamma \sim eV/(m_e c^2)$ during outburst than are found for the slowly decaying, quasi-steady state magnetosphere in Section 4.

The plasma frequency at the electron density (7) exceeds the frequency of the observed radiation, and in a current sheet carrying the current density (19) it is orders of magnitude greater still. Despite this, it is possible for radiation at the observed frequencies to be emitted because the dense plasma, and radiation source, is confined on magnetic surfaces with an abrupt density discontinuity; surface charges and currents of this overdense plasma are the sources of radiation, which does not propagate through the plasma itself.

Curvature radiation has been suggested as the emission mechanism of radio pulsars (Ghosh 2007; Melrose & Yuen 2016), with their high brightness temperature requiring, and explained by, clumping (correlation) of the radiating electrons. Curvature radiation may also explain their linear and circular polarization (Gil & Snakowski 1990; Ganjadhara 2010; Kumar & Ganjadhara 2012; Wang et al. 2014). The subject remains controversial.

In analogy, curvature radiation might account for the radio emission of FRBs. An argument in favor of this hypothesis is the observation of both linear (Masui et al. 2015) and circular (Petroff et al. 2015) polarization in FRBs, though in different events. However, at the Lorentz factors estimated during outburst (23), curvature radiation would occur at frequencies far in excess of those observed in FRBs.

7. SUMMARY AND CONCLUSION

Several lines of argument, including energetics, comparison of event rates with those of other transients such as SNRs and GRBs, and the energy emitted as an accreting or despinning neutron star approaches its stability limit indicate that FRBs are not produced by one-time catastrophic events. This conclusion is supported by the discovery (Thornton 2013; Champion et al. 2015) of a double-pulsed FRB with subpulse separation (about 2 ms) greater than the neutron star collapse time, indicating two distinct events produced by the same source, and recently confirmed (Spitler et al. 2016). In such models, FRBs may repeat, breaking any connection between their observed rate and the birth rate of their parent objects.

This suggests that FRBs are associated with other brief transients. If FRBs are at the "cosmological" distances indicated by their dispersion measures, giant PSR pulses (including RRAT) cannot be sufficiently energetic unless the neutron star is both extremely fast-rotating and strongly magnetized. This combination is not observed among Galactic pulsars and is almost self-contradictory, because strong magnetic fields lead to rapid spindown. The remaining category of known brief electromagnetic transients is the SGR. The rate of Galactic giant SGR flares exceeds the observed rate of FRBs per galaxy by several orders of magnitude if FRBs are at "cosmological" distances, but there are several possible explanations, of which the most obvious is that only a small fraction of SGR-associated FRBs are energetic enough to be observable at those distances.

Consideration of possible mechanisms for dissipation of magnetostatic energy in transparent regions, as required by the fast (sub-millisecond) timescales of both FRBs and the rising phase of giant SGR flares, points toward currents flowing on magnetospheric arches, analogous to solar coronal arches. Such arches have lifetimes of thousands of years or less, depending on the magnitude of the magnetic field, and may explain why SGR/AXP behavior is found in young, high-field neutron stars, and why neutron stars that are either older or have smaller fields may be radio pulsars, but are not SGRs/AXPs. The criterion is the ratio of field to age, explaining why older neutron stars do not show SGR/AXP activity even if their

fields are in the "magnetar" range (Manchester et al. 2005), as well as younger, but lower, field neutron stars like the Crab pulsar.

I hypothesize that SGR/AXP and FRB activity requires the persistence of magnetospheric currents. Their decay time τ (Equation (12)) for neutron stars with the highest magnetic fields is consistent with estimated SGR/AXP ages. The smaller values of τ for neutron stars with lower fields (such as the Crab pulsar) explain why they are not SGRs/AXPs, even when they are younger than observed SGRs/AXPs. Magnetospheric currents have also decayed in older pulsars, even those with fields in the "magnetar" range (McLaughlin et al. 2003; Manchester et al. 2005), explaining why they too are not SGRs/AXPs.

Some possible alternative hypotheses and the non-detection of an FRB accompanying SGR 1806-20 are discussed in the appendices.

APPENDIX A
COMPTON RECOIL OF ANNIHILATION RADIATION

In the latter ($\gtrsim$1 ms) part of an SGR flare, its pair plasma thermalizes, radiating the characteristic soft SGR spectra, but during their rapid ($<$1 ms) rising phase, more energetic pair annihilation gamma-rays (a tiny fraction of the total energy radiated) may be produced, such as those that were reported from SGR 0525–66 (Cline 1980; Cline et al. 1980). These gamma-rays Compton scatter in surrounding plasma, creating a broadly directed flow of semi-relativistic electrons for which the distribution function peaks at the highest kinematically permitted energy. This excites the "bump-on-tail" plasma instability in a background plasma (Beloborodov & Demianski 1995).

A.1. Distribution Function

Annihilation radiation Compton scatters on non-relativistic plasma, producing a broad beam of recoiling electrons. In the simplest possible case, the annihilation spectrum is monochromatic with $h\nu = m_e c^2 = 511$ keV, the target electron distribution is "cold," with negligible (compared to c) thermal velocities, the target is sufficiently distant from the source that the photons can be considered a directed beam and the effects of magnetic fields are ignored (valid if $B \ll m_e c^3/e\hbar = 4.4 \times 10^{13}$ Gauss and B is parallel to the photon beam). The differential scattering cross-section is given by the Klein–Nishina formula (Bjorken & Drell 1964)

$$\frac{d\sigma}{d\Omega} = \frac{e^4}{2m_e^2 c^4}\left(\frac{\nu'}{\nu}\right)^2\left(\frac{\nu'}{\nu} + \frac{\nu}{\nu'} - \sin^2\theta\right), \tag{24}$$

where the frequencies of the incident and scattered photons are ν and ν'. Kinematics dictates a relation between the direction of the scattered electron and its energy

$$\nu' = \frac{\nu}{1 + (2h\nu/m_e c^2)\sin^2(\theta/2)}. \tag{25}$$

Plasma instability depends on the component of electron velocity parallel to the wave vector of the plasma oscillation, so consider only the component of velocity parallel to the incident photon beam. The resulting distribution function of scattered electrons is shown in Figure 2.

The distribution function $f(\theta, v)$ of scattered electrons evolves as a result of Coulomb drag on the much larger population of unscattered electrons and of ions. This is described by a Fokker–Planck equation

$$\frac{\partial f(\theta, v)}{\partial t} = S(\theta, v) - \frac{\partial}{\partial v}\left(\frac{dv}{dt} f(\theta, v)\right), \tag{26}$$

where S is the scattering source function and $dv/dt \propto \beta^{-2}\gamma^{-3}$ represents Coulomb drag (slowing by loss of energy to background plasma; Gould 1972). In steady state, this reduces to

$$f(\theta, v) = C\beta^2\gamma^3 \int_{v'=v}^{\infty} S(\theta, v')dv', \tag{27}$$

where $\beta \equiv v/c$ and $\gamma \equiv (1 - \beta^2)^{-1/2}$. Here $\boldsymbol{v}$ is the velocity vector and v the speed; θ remains constant during slowing (aside from a small amount of straggling), so $f(\theta, v)$ may be evaluated independently for each θ and the three-space speed projected onto the beam direction.

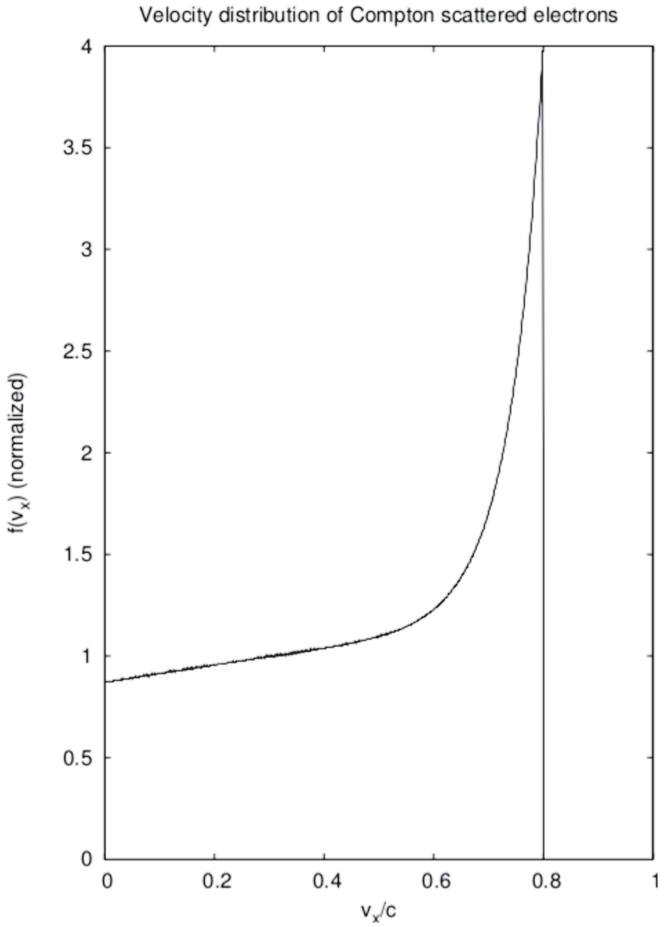

Figure 2. Normalized distribution function vs. velocity component in the beam direction of electrons Compton scattered by a beam of 511 keV photons.

A.2. Plasma Instability

A multipeaked electron distribution function $f(v_x)$, such as that shown in Figure 2 with the addition of the thermal electron peak at small velocity (not in the figure, that only shows the scattering source) is unstable to the electrostatic "bump-on-tail" instability. This instability is essentially inverse Landau damping, and occurs whenever the derivative of the distribution function with respect to some component of electron

velocity is positive. Electron plasma waves with phase velocities $v_{\rm ph} = \omega/k$ (ω and k are the plasma wave frequency and wave vector, related by the dispersion relation $\omega^2 = \omega_p^2 + 3k^2\lambda_D^2$, where ω_p is the plasma frequency and λ_D the Debye length) for which $\partial F_0(v_x)/\partial v_x|_{v_x=v_{\rm ph}} > 0$ grow at a rate of (Chen 1974)

$$\gamma = \frac{\pi}{2}\frac{\omega_p^3}{k^2}\frac{n_{\rm beam}}{n_e}\frac{\partial F_0(v_x)}{\partial v_x}\Bigg|_{v_x=\omega/k}, \quad (28)$$

where $F_0(v_x)$ is the normalized one-dimensional electron distribution function of a density $n_{\rm beam}$ of high velocity (Compton recoil) electrons and n_e is the background electron density. If the fast electrons are only a small fraction of the total electron density and their speeds are much greater than the electron thermal velocity, conditions that are generally met, then for waves excited by the fast electrons $\omega \approx \omega_p$ and $k \approx \omega_p/v$, where v is a velocity on the rising part of the electron distribution function. Then the growth rate becomes

$$\frac{\pi}{2}\frac{\omega_p v^2}{n_e}\frac{\partial f(v_x)}{\partial v_x}\Bigg|_{v_x=\omega/k}, \quad (29)$$

where $f(v_x)$ is not normalized to $n_{\rm beam}$, but is the full electron distribution function.

The rapid decrease of drag deceleration with increasing speed, shown by the factor $\beta^2\gamma^3$ in Equation (27), acts to create a minimum in $f(v_x)$ (the large peak in $f(v_x)$ from thermal electrons at very small velocity is not shown in Figure 2) even when $S(v)$ is a monotonically decreasing function, as it can be for power-law photon spectra or a mixture of two- and three-photon annihilation (not shown). For example, if $S(v) \propto v^{-n}$, making the non-relativistic approximation $\gamma \to 1$, then $f(v) \propto v^{3-n}$. For all but the most steeply decreasing $S(v)$, $n < 3$ and $f'(v) > 0$ for v exceeding a few thermal velocities, and the plasma is unstable. In the opposite limit of scattering by very energetic gamma-rays $S(v) \to \delta(v - c)$, $f(v) \propto v^2\gamma^3$, $f'(v) > 0$ and again the plasma is unstable (for quantitative growth rates Equations (28) and (29) need to be corrected for the relativistic increase in electron mass).

This mechanism of producing unstable electron distributions may operate anywhere an intense flux of gamma-rays, not necessarily from positron annihilation, whose spectrum is not too steep, is incident upon a non-relativistic plasma. The required intensity is determined by the competition between the growth rate γ (Equations (28) and (29)), proportional to the gamma-ray flux, and the collisional damping rate of the plasma wave that depends on the plasma density and temperature.

For a plasma frequency comparable to the frequencies $\approx$1400 MHz of observed FRBs, $n_{\rm beam} \gtrsim 10^{-6} n_e$ is sufficient to grow the instability by $\sim$10 e-folds to saturation in the sub-millisecond timescale of FRBs.

A.3. Energetic Failure

This apparently attractive model fails on energetic grounds. The total Klein–Nishina cross-section for a 511 keV photon is 2.85×10^{-25} cm^2, so that annihilation radiation will penetrate a plasma to a depth of about 4×10^{24} electrons cm^{-2}. If electrons receive an average energy of $m_e c^2$ the total deposited energy is about 3×10^{18} erg cm^{-2}. If more energy were deposited the electron thermal energies would be $\gtrsim m_e c^2$, their distribution function would not be inverted ($\partial f(v_x)/\partial v_x$ would be negative at all v_x) and there would be no instability. Over a hemisphere of a neutron star, the total deposited energy must be less than 10^{31} erg, failing to account for observed FRB energies, even assuming perfectly efficient radiation, by nine orders of magnitude.

An even stronger conclusion results from noting that the critical density for the observed 1.4 GHz FRB radiation, above which it cannot propagate, is $n_e = 2.4 \times 10^{10}$ cm^{-3}. A magnetosphere filled with that density of semi-relativistic plasma would contain less than 10^{23} erg of plasma energy.

APPENDIX B
POSSIBLE ALTERNATIVES TO SGR?

A number of alternative sites of FRBs have been considered, in most cases without detailed modeling of the emission mechanisms. Here I discuss two such sites that, like SGRs, involve neutron stars, and point out significant unresolved questions.

B.1. Giant Pulsar Pulses

The "nanoshots" of a few radio pulsars are even shorter than FRBs, with durations of nanoseconds (Soglasnov et al. 2004; Hankins & Eilek 2007), but involve energies smaller than those of FRBs by many orders of magnitude. In fact, their instantaneous radiated power, even during their nanosecond peaks, is less than their pulsars' mean spin-down power. This supports the hypothesis that, as in classical pulsar theory (Gold 1968; Goldreich & Julian 1969; Ghosh 2007), they do not tap stored magnetic energy.

Giant pulsar pulses have been suggested (Connor et al. 2016; Cordes & Wasserman 2016) as the origin of FRBs. If their instantaneous power is less than their mean spin-down power (no release of stored magnetostatic energy), as is always the case for Galactic radio pulsars, then the inferred luminosity of at least one FRB at "cosmological" distances ($L_{\rm FRB} \gtrsim 10^{43}$ erg s^{-1}; Thornton et al. 2013) precludes explaining FRBs as giant pulsar pulses unless the neutron stars are rotating near breakup and are very strongly magnetized and hence very young. Their ages must be $< E_{\rm rot}/L_{\rm FRB} \sim 100$ year, where $E_{\rm rot} \approx 5 \times 10^{52}$ erg is the rotational energy of a neutron star at its rotational limit. If intrinsic FRB pulse widths are shorter than 1 ms (the observational upper limit), then $L_{\rm FRB}$ is correspondingly greater and the upper bound on the age of the most luminous FRBs is correspondingly less.

The existence of such high-field millisecond pulsars would not violate any law of physics, and Ostriker & Gunn (1971) suggested that they make supernovae. However, they have never been observed, may lead to a conflict between SN and FRB rates (supernova remnant energies and the absence of pulsars in most SNRs indicate that they can only be an unusual subclass of neutron star births) and cannot explain the distribution of FRB dispersion measures (Katz 2016).

B.2. Neutron Star Collapse

The collapses of *accreting* NSs cannot be the explanation of FRBs. Most neutron stars are observed to have masses of about 1.4 $M_\odot$, but the maximum mass of neutron stars must be at least 2.0 $M_\odot$ because a few such massive neutron stars are known. For accretion to push a 1.4 $M_\odot$ neutron star to collapse would require the release of at least $\sim$0.6 $M_\odot(GM/r) \approx 10^{53}$ erg; and

one such event per 1000 years in a galaxy implies a mean X-ray emission of about 3×10^{42} erg s^{-1}. This is about 10^3 times the 2–10 keV X-ray luminosity of our Galaxy (Grimm et al. 2002). Only if these hypothetical progenitors of FRBs are born very close (within $\sim 10^{-3} M_\odot$) to their stability limit can the FRB rate be reconciled with the observed bounds on galactic X-ray emission. This argument would not exclude the collapse of rotationally stabilized (not accreting) NSs as the result of angular momentum loss (Falcke & Rezzolla 2014) if they, like recycled pulsars, are inefficient ($\mathcal{O}(10^{-3}$–$10^{-4})$ Bogdanov et al. 2006) X-ray emitters. However, their mechanism of emission of an FRB remains obscure; the timescale of collapse (and disappearance of the NS magnetic moment) would be 10^{-4}–10^{-5} s, corresponding to emission at tens of kHz, not the observed frequencies $\sim$1 GHz.

APPENDIX C
SGR 1806-20

Tendulkar et al. (2016) found that the Parkes telescope was observing a pulsar at the time of the giant 2004 December 27 outburst of SGR 1806-20, and that the SGR was 31°.5 above the horizon and 35°.6 away from the beam direction. Analysis of the data found no evidence of an FRB, with an upper limit tens of dB lower than predicted for a Galactic FRB out of beam (Katz 2014, 2016). This appears to contradict the suggestion that FRB and SGR outbursts are associated, but possible explanations should be considered.

Atmospheric absorption: SGR 1806-20 deposited about 1 erg cm^{-2} of soft (30–100 keV) gamma-rays into the Earth's atmosphere at a depth of roughly 5 g cm^{-2}, where the molecular density is about 2×10^{17} cm^{-3}. Approximately 2×10^{10} electrons are produced per erg of deposited energy, mostly distributed over a single scale height, and their recombination or capture time is long. Because of the high density, their collision rate (with neutral molecules) is high, absorbing energy from a propagating radio-frequency pulse. A rough calculation indicates an optical depth of about 0.02 for 1.4 GHz radiation, which is insignificant.

Absorption at source: SGR 1806-20 emitted at least 10^{46} erg of soft gamma-rays, or about 2×10^{53} photons. Some of these may be absorbed in a dense surrounding cloud, and if the cloud density exceeds 10^5 cm^{-3} the $\sim$30 keV photoelectrons will each produce an additional $\sim$1000 electrons by collision in the $\sim$1 s SGR duration. Such a cloud, with DM $\gtrsim$300 pc cm^{-3}, could be an effective absorber of $\sim$1 GHz radiation, but only if it were close enough to the SGR (within $\sim 3 \times 10^{15}$ cm) to be fully ionized. Such a dense cloud that close to a neutron star, within an SNR, is implausible. In addition, only a fraction $\lesssim 10^{-2}$ of the energy of the $\sim$100 ms SGR flare is emitted in its $\lesssim$1 s rising edge assumed to correspond to the brief FRB.

Propagation broadening: Tendulkar et al. (2016) consider scattering (multipath) pulse broadening timescales in the range of 14–56 ms, a range suggested by pulsar-derived models of interstellar propagation. However, Krishnakumar et al. (2015) found that the most highly dispersed pulsars have broadenings of about 6×10^4 ms at 327 MHz, scaling ($\propto \nu^{-4.4}$) to about 100 ms at the frequency of observation of Tendulkar et al. (2016). Pulsar searches are strongly biased against detection of highly broadened pulses and may be blind to highly dispersed objects, so gamma-ray selected objects in the Galactic plane (such as SGRs) may be much more broadened than those discovered in pulsar surveys. Perhaps a radio burst from SGR 1806-20 was so broadened as not to have been detectable after filtering for pulsar-like rapid time variability.

Rejection as interference: a strong source far out of beam produces signals of similar amplitude in each of Parke's 13 beams. This is also a characteristic of interference (from local sources, or entering amplifiers by their "back doors"), and such signals may have been rejected as likely interference.

Tendulkar et al. (2016) also compare the FRB rate to that of short GRBs, a fraction $f < 0.15$ of which have been suggested (Nakar et al. 2006; Ofek 2007) to actually have been SGRs. Because of the comparatively low sensitivity of gamma-ray detectors, if these short GRBs are associated with giant SGR outbursts at a ratio of 1:1, then comparison of the event rates indicates that they are detected only to a distance cutoff (assuming homogeneous distributions in Euclidean geometry) $0.013(f/0.15)^{1/3}$ of the FRB distance cutoff. If the latter is at $z = 1$, then the cutoff on SGR detection is about $55(f/0.15)^{1/3}$ Mpc, and a nominal gamma-ray fluence sensitivity of 10^{-8} erg cm^{-2} would correspond to an (isotropic) SGR energy of $4 \times 10^{45}(f/0.15)^{2/3}$ erg. This is consistent with measurements of Galactic SGR, but the uncertainty in f and in the effective detector sensitivity make this a crude comparison.

Note added in proof. A result similar to (10) has been obtained by Beloborodov & Li (2016).

REFERENCES

Akgün, T., Miralles., J. A., Pons, A., & Cerdá-Durán, P. 2016, arXiv:1605.02253
Bak, P., Tang, C., & Wiesenfeld, K. 1987, PhRvL, 59, 381
Beloborodov, A. M. 2009, ApJ, 703, 1044
Beloborodov, A. M., & Demianski, M. 1995, PhRvL, 74, 2322
Beloborodov, A. M., & Li, X. 2016, arXiv:1605.09077
Beloborodov, A. M., & Thompson, C. 2007, ApJ, 657, 967
Bjorken, J. D., & Drell, S. D. 1964, Relativistic Quantum Mechanics (New York: McGraw-Hill)
Bogdanov, S., Grindlay, J. E., Heinke, C. O., et al. 2006, ApJ, 646, 1104
Champion, D. J., Petroff, E., Kramer, M., et al. 2015, arXiv:1511.07746
Chen, F. F. 1974, Introduction to Plasma Physics (New York: Plenum)
Cline, T. L. 1980, ComAp, 9, 13
Cline, T. L., Desai, U. D., Pizzichini, G., et al. 1980, ApJL, 237, L1
Connor, L., Sievers, J., & Pen, U.-L. 2016, MNRAS, 458, L19
Cordes, J. M., & Wasserman, I. 2016, MNRAS, 457, 232
Davis, L. 1947, PhRv, 72, 632
Falcke, H., & Rezzolla, L. 2014, A&A, 562, 137
Fishman, G. J., Meegan, C. A., Wilson, R. B., et al. 1994, ApJS, 92, 229
Ganjadhara, R. T. 2010, ApJ, 710, 29
Ghosh, P. 2007, Rotation and Accretion Powered Pulsars (Singapore: World Scientific)
Gil, J. A., & Snakowski, J. K. 1990, A&A, 234, 237
Gold, T. 1968, Natur, 218, 731
Goldreich, P., & Julian, W. H. 1969, ApJ, 157, 869
Gould, R. J. 1972, Phy, 60, 145
Grimm, H.-J., Gilfanov, M., & Sunyaev, R. 2002, A&A, 391, 923
Hankins, T. H., & Eilek, J. A. 2007, ApJ, 670, 693
Heisenberg, W., & Euler, H. 1936, ZPhy, 98, 714
Hones, E. W., & Bergeson, J. E. 1965, JGR, 70, 4951
Hurley, K., Boggs, S. E., Smith, D. M., et al. 2005, Natur, 434, 1098
Hurley, K., Cline, T., Mazets, E., et al. 1999, Natur, 397, 41
Jackson, J. D. 1962, Classical Electrodynamics (New York: Wiley)
Katz, J. I. 1982, ApJ, 260, 371

Katz, J. I. 1986, JGR, 91, 10412
Katz, J. I. 1996, ApJ, 463, 305
Katz, J. I. 2014, PhRvD, 89, 103009
Katz, J. I. 2016, ApJ, 818, 19
Krishnakumar, M. A., Mitra, D., Naidu, A., Joshi, B. C., & Manoharan, P. K. 2015, ApJ, 804, 23
Kulkarni, S. R., Ofek, E. O., & Neill, J. D. 2015, arXiv:1511.09137
Kulkarni, S. R., Ofek, E. O., Neill, J. D., Zhang, A., & Juric, M. 2014, ApJ, 797, 70
Kumar, D., & Ganjadhara, R. T. 2012, ApJ, 746, 157
Laros, J. G., Fenimore, E. E., Klebesadel, R. W., et al. 1987, ApJL, 320, L111
Law, C. J., Bower, G. C., Burke-Spolaor, S., et al. 2015, ApJ, 807, 16
Lyubarsky, Y. 2014, MNRAS, 442, L9
Lyutikov, M. 2006, MNRAS, 367, 1594
Lyutikov, M. 2013, arXiv:1306.2264
Manchester, R. N., Hobbs, G. B., Teoh, A., & Hobbs, M. 2005, AJ, 129, 1993
Masui, K., Lin, H.-H., Sievers, J., et al. 2015, Natur, 528, 523
Mazets, E. P., Golenetskii, S. V., & Gur'yan, Yu. A. 1979, SvAL, 5, 343
McLaughlin, M. A., Stairs, I. H., Kaspi, V. M., et al. 2003, ApJL, 591, L135
Melrose, D. B., & Yuen, R. 2016, arXiv:1604.03623
Nakar, E., Gal-Yam, A., Piran, T., & Fox, D. B. 2006, ApJ, 640, 849
Ofek, E. O. 2007, ApJ, 659, 339
Ostriker, J. P., & Gunn, J. E. 1971, ApJL, 164, L95
Palmer, D. M., Barthelmy, S., Gehrels, N., et al. 2005, Natur, 434, 1107
Parker, E. N. 1979, Cosmical Magnetic Fields: Their Origin and Their Activity (Oxford: Oxford Univ. Press)
Pen, U.-L., & Connor, L. 2015, ApJ, 807, 179
Petroff, E., Bailes, M., Barr, E. D., et al. 2015, MNRAS, 447, 246
Popov, S. B., & Postnov, K. A. 2007, arXiv:0710.2006
Popov, S. B., & Postnov, K. A. 2013, arXiv:1307.4924
Priest, E., & Forbes, T. 2000, Magnetic Reconnection (Cambridge: Cambridge Univ. Press)
Qin, Y., Liang, E.-W., Liang, Y.-F., et al. 2013, ApJ, 763, 15
Schwinger, J. 1951, PhRv, 82, 664
Soglasnov, V. A., Popov, M. V., Bartel, N., et al. 2004, ApJ, 616, 439
Spitler, L. G., Scholz, P., Hessels, W. T., et al. 2016, arXiv:1603.00581
Stebbins, A., & Yoo, H. 2015, arXiv:1505:06400
Tendulkar, S. P., Kaspi, V. M., & Patel, C. 2016, arXiv:1602.02188
Thompson, C., & Duncan, R. C. 1992, ApJL, 392, L9
Thompson, C., & Duncan, R. C. 1995, MNRAS, 275, 255
Thompson, C., Lyutikov, M., & Kulkarni, S. R. 2002, ApJ, 574, 332
Thornton, D. 2013, PhD thesis, Univ. Manchester
Thornton, D., Stappers, B., Bailes, M., et al. 2013, Sci, 341, 53
Wang, P. F., Wang, C., & Han, J. L. 2014, MNRAS, 441, 1943
Widrow, L. M. 2002, RvMP, 74, 775